

## Neutron resonance spectroscopy: $^{203, 205}\text{Tl}^\dagger$

H. I. Liou,\* J. Rainwater, G. Hacken, and U. N. Singh

Columbia University, New York, New York 10027

(Received 19 March 1975)

Results are presented for high resolution time of flight neutron spectroscopy measurements of samples of natural Tl metal and of samples enriched in  $^{203}\text{Tl}$  and in  $^{205}\text{Tl}$ . Plots of  $\sigma_t$  vs  $E$  are given to 160 keV. Below 20 keV all observed levels are identified by isotope, and as  $s$  or  $p$ , the orbital angular momentum of the interacting neutron. Values of  $E_0$  and  $g\Gamma_n$  are given for all observed levels, comprised of 25  $s$  and 11  $p$  levels in  $^{203}\text{Tl}$ , and 5  $s$  and 6  $p$  levels in  $^{205}\text{Tl}$ . Favored  $J$  is given in many cases. Values of  $\Gamma_\gamma$  for 6  $s$  levels in  $^{203}\text{Tl}$  and 2  $s$  levels in  $^{205}\text{Tl}$  give  $\langle\Gamma_\gamma\rangle = 0.65$  eV for  $^{203}\text{Tl}$  and 0.80 eV for  $^{205}\text{Tl}$ . Above 20 keV, values of  $E_0$  and  $\Gamma$  ( $\approx \Gamma_n$ ) are given for 29  $s$  levels to 104 keV, with favored  $A$  for 20 levels and favored  $J$  for 16 levels. Values of  $E_0$  and ( $ag\Gamma_n$ ) are given for 44  $p$  levels above 20 keV. Intermediate structure effects seem to be present for  $^{203}\text{Tl}$  to give  $\sum g\Gamma_n^0/\Delta E$  below 6.6 keV much larger than for  $6.6 \text{ keV} < E < 20 \text{ keV}$ . Ignoring that effect, a usual analysis for the results below 20 keV gives  $10^4 S_0 = (1.28 \pm_{-0.31}^{+0.45})$  for  $^{203}\text{Tl}$  and  $(0.38 \pm_{-0.16}^{+0.44})$  for  $^{205}\text{Tl}$ , with  $10^4 S_1 = (0.25 \pm_{-0.09}^{+0.13})$  for  $^{203}\text{Tl}$  and  $(0.15 \pm_{-0.07}^{+0.14})$  for  $^{205}\text{Tl}$ .

[ NUCLEAR REACTIONS  $^{203, 205}\text{Tl}(n, n)$ ,  $(n, \gamma)$ ,  $E = 15 \text{ eV} - 104 \text{ keV}$ ; measured  $\sigma_t(E)$  to 160 keV; deduced  $E_0$ ,  $l$ ,  $J$ ,  $g\Gamma_n$  or  $ag\Gamma_n$  or  $\Gamma$ ,  $S_0$ ,  $S_1$ . ]

### I. INTRODUCTION

This is one of a series<sup>1-19</sup> of papers reporting results of high resolution neutron time of flight spectroscopy measurements using the Columbia University Nevis synchrocyclotron as a pulsed neutron source. Results are presented from 202.05 m transmission measurements and 39.57 m capture measurements using samples of natural Tl and samples isotopically enriched in  $^{203}\text{Tl}$  or  $^{205}\text{Tl}$ . Below 20 keV, all resonances seen in a thick natural Tl sample are identified as due to  $^{203}\text{Tl}$  (25  $l=0$  and 11  $l=1$  levels) or  $^{205}\text{Tl}$  (5  $l=0$  and 6  $l=1$  levels) with the resonance  $J$  values (0 or 1) established for most  $s$  levels, and  $g\Gamma_n$  values given for all levels. Between 20 and 104 keV, we see 29  $s$  levels and 44  $p$  levels, obtaining the isotope identification for 18  $s$  levels and the resonance  $J$  values for 14  $s$  levels. Values of  $\Gamma \approx \Gamma_n$  are given for all  $s$  levels, with  $ag\Gamma_n$  given for all  $p$  levels. In addition, eight levels were seen between 71 and 87 keV which are too crowded to permit satisfactory evaluation of  $A$ ,  $l$ ,  $J$ , or  $ag\Gamma_n$  values.

Thallium is interesting in that it is near both proton and neutron closed shell numbers (82 and 126) for the compound nuclei. Near closed shells it is observed and expected that  $s$  level densities decrease dramatically from those for nearby nuclei further from closed shell values. Although the binding energies of an extra neutron to  $^{203}\text{Tl}$  and  $^{205}\text{Tl}$  are nearly equal, 6.6558 and 6.5039 MeV, much higher  $s$  level density is seen for  $^{203}\text{Tl}$  than

for  $^{205}\text{Tl}$ . Both compound nuclei  $Z$  values are one less than closed shell 82, but  $^{204}\text{Tl}$  has  $(126 - N) = 3$ , vs 1 for  $^{206}\text{Tl}$ . Intermediate structure due to doorway states is expected mainly near closed shell ( $Z, N$ ) values. A plot of  $\sum g\Gamma_n^0$  for  $s$  levels in  $^{203}\text{Tl}$  shows fluctuations greater than expected statistically for a single channel process with constant  $\langle g\Gamma_n^0 \rangle$  vs  $E$  over the energy interval studied.

Level strengths have previously only been given<sup>20</sup> for the  $^{203}\text{Tl}$  levels at 38 and 239 eV. Newson *et al.*<sup>21</sup> report resonance energies for eight levels from 1.2 to 29 keV, without giving level widths. Their energy resolution was too poor for their reported energies to be correlated with our level energies for the 23  $s$  levels and 8  $p$  levels which we see between 1 and 20 keV. The main previously reported results for  $^{205}\text{Tl}$  are due to Earle *et al.*<sup>22,23</sup> using the Oak Ridge electron linear accelerator (ORELA) for resonance capture measurements. While they state that most resonances were resolved below 250 keV, level strengths are only given for four levels from 1 to 32 keV. They give level energies for 31 levels in  $^{205}\text{Tl}$  between 2.7 and 33 keV. We do not observe about half of the  $^{205}\text{Tl}$  levels of their list to 33 keV so the levels which we miss are quite weak. Below 20 keV we rely on their  $^{205}\text{Tl}$  level list to establish as due to  $^{203}\text{Tl}$  or  $^{205}\text{Tl}$  all levels seen in our thick natural Tl sample, but not identified by isotope in our separated isotope data. Above 20 keV, we did not use their list because of significant differences between their and our energies which made

the correspondence uncertain.

The detailed analysis of this data is mainly due to H. I. Liou.

## II. EXPERIMENTAL DETAILS AND ANALYSIS PROCEDURES

The measurements for Tl were made during the same cyclotron "run" as those for the nuclei for which results have been reported in Refs. 3, 7, 8, 11-15, and 18. A detailed description of the experimental system operation was given in Refs. 1 and 3. The neutron energy spectrum was covered using 16 000 detection channels. For the 202.05 m transmission measurements, 40 ns detection channel widths were used for  $E > 1280$  eV, with progressively increasing widths to 1280 ns at 15 eV. The 39.57 m resonance capture measurements used 40 ns widths above 306 eV, followed by 80 ns widths to the lowest observed energy level near 37 eV.

For the transmission measurements, a single thickness natural Tl sample (29.5%  $^{203}\text{Tl}$ , 70.5%  $^{205}\text{Tl}$ ) was used having  $(1/n) = 8.14$  b/atom. A sin-

gle thinner natural Tl sample,  $(1/n) = 74.0$  b/atom, was used for the capture measurements. For both capture and transmission measurements, two thicknesses of enriched  $^{203}\text{Tl}_2\text{O}_3$  were used having  $(1/n) = 356$  and 1060 b/atom of  $^{203}\text{Tl}$ . The sample was 96.69%  $^{203}\text{Tl}$  and 3.31%  $^{205}\text{Tl}$ . A single enriched  $^{205}\text{Tl}_2\text{O}_3$  sample was used having 1%  $^{203}\text{Tl}$  and 99%  $^{205}\text{Tl}$  with  $(1/n) = 269$  b/atom of  $^{205}\text{Tl}$ . About four million cyclotron operation bursts ( $\sim 16$ h) were devoted to counting with Tl samples in the beam, giving  $> 8 \times 10^7$  total detector counts.

The background subtractions for the thick natural Tl sample were made easy by many "bottoming transmission dips" ( $T \approx 0$ ). The thicker  $^{203}\text{Tl}$  sample transmission had a few "bottoming transmission dips" which permitted accurate background subtractions to be made for the separated isotope sample data, and for the "open beam" data ( $T = 1$  reference). The separated isotope capture data were useful for isotope identification of levels. The separated isotope transmission data helped both for isotope identification of levels and for establishing the level strengths and  $J$  values.

After the background subtractions had been made,

TABLE I. Resonance parameters for  $^{203}\text{Tl}$  and  $^{205}\text{Tl}$  below 20 keV. All levels listed were seen in the thick natural Tl transmission data. The isotope identification for levels with no symbol before the energy is from our separated isotope results. Levels labeled \* have their isotope identification from Ref. 20. The  $^{203}\text{Tl}$  levels labeled ‡ are classified as due to  $^{203}\text{Tl}$  since they were not in the list of  $^{205}\text{Tl}$  levels in Ref. 22.

$E_0$ (eV)	$g\Gamma_n$ (eV)	$J$	$l$	$E_0$ (eV)	$g\Gamma_n$ (eV)	$J$	$l$
$^{203}\text{Tl}$							
* 37.91 ± 0.11	0.000 019 ± 0.000 006		1	5397.0 ± 2.2	5.1 ± 0.7	1	0
238.0 ± 1.6	3.0 ± 0.3	1	0	5813.7 ± 2.5	1.4 ± 0.2	1	0
‡ 539.73 ± 0.28	0.0024 ± 0.0005		1	6334.2 ± 2.8	4.2 ± 0.6	1	0
842.00 ± 0.54	0.28 ± 0.02	1	0	6598.5 ± 5.9	12 ± 2	0	0
‡ 995.50 ± 0.34	0.0076 ± 0.0020		1	7421.8 ± 3.5	0.45 ± 0.15		1
1130.0 ± 3.9	11 ± 2	0	0	8521.6 ± 4.4	1.1 ± 0.4		0
1275.2 ± 0.5	0.53 ± 0.10		0	‡ 9187.1 ± 4.9	0.43 ± 0.14		1
1328.5 ± 0.5	0.13 ± 0.03		0	9363.0 ± 5.0	4.0 ± 1.0	(0)	0
1433.2 ± 1.2	2.1 ± 0.2	1	0	10 986 ± 7	3.3 ± 0.8	0	0
‡ 1917.9 ± 0.9	0.016 ± 0.005		1	12 381 ± 8	14 ± 2	1	0
2002.4 ± 1.0	0.018 ± 0.005		1	12 627 ± 8	4.8 ± 1.0	0	0
2790.7 ± 0.9	2.7 ± 0.3	1	0	12 923 ± 9	15 ± 4	1	0
3587.6 ± 1.2	0.069 ± 0.017		1	‡ 14 867 ± 10	0.76 ± 0.25		1
3736.5 ± 1.3	4.3 ± 0.5	0	0	‡ 15 122 ± 11	4.9 ± 2.0		0
4391.3 ± 3.2	16 ± 2	0	0	16 292 ± 12	26 ± 6		0
4658.5 ± 3.5	11 ± 2	1	0	17 330 ± 13	33 ± 8		0
‡ 5038.1 ± 3.9	0.11 ± 0.04		1	17 999 ± 14	8.4 ± 4.0		0
‡ 5319.6 ± 4.3	0.19 ± 0.07		1	19 231 ± 15	16 ± 3	0	0
$^{205}\text{Tl}$							
* 44.61 ± 0.06	0.000 024 ± 0.000 006		1	* 11 757 ± 7	0.53 ± 0.17		1
2793.5 ± 0.9	1.1 ± 0.2		0	* 13 254 ± 9	0.80 ± 0.25		1
3039.0 ± 1.0	3.7 ± 0.5	1	0	16 523 ± 24	37 ± 8		0
5098.4 ± 2.0	0.45 ± 0.10	0	0	17 443 ± 13	30 ± 15		0
8436.0 ± 4.3	0.20 ± 0.05		1	* 18 651 ± 14	2.2 ± 0.8		1
* 10 182 ± 6	0.63 ± 0.20		1				

TABLE II. Resonance parameters for Tl  $l=0$  levels above 20 keV. The levels with † labeled before the  $A$  have their isotope identification from our separated isotope results, while for the other cases, the favorable  $A$  is from the best choice of ( $ag$ ) for our single level shape fitted to the thick natural sample transmission data which includes the interference between potential and resonance scattering. The  $ag$  values are 0.074 ( $J=0, 203$ ), 0.221 ( $J=1, 203$ ), 0.176 ( $J=0, 205$ ), and 0.529 ( $J=1, 205$ ). Label D indicates that the level may be a doublet.

$E_0$ (eV)	$\Gamma$ (eV)	$A$	$J$	$E_0$ (eV)	$\Gamma$ (eV)	$A$	$J$
20235±16	10± 3	203	0	32 877± 33	95± 40		
20 756±17	18± 4	203	1	D 33 490± 34	220± 50	†203	0
		205	0	39 200± 43	120± 30	203	0
D21 983±18	65±25	†203		41 920± 47	90± 20	203	1
D23 327±20	80±30	†203		D 45 498± 53	300± 80	†203	
24 035±21	32±14			47 474± 57	120± 70		
24 830±22	60±20	203	0	50 500± 63	480± 40	†205	1
25 760±23	35±10	203	0	54 250± 70	220± 30	†205	0
28 180±26	70±20	203	0	62 345± 86	450±250		
29 366±28	50±20			65 302± 92	550±300		
29 728±28	48±18			67 440± 96	200± 50	205	0
31 120±30	70±25	†205	0	D 68 950±100	280±100		
31 379±31	110±50	†203		83 990±140	500±300		
31 960±32	40±15	†203	1	93 000±160	700±100	205	1
32 633±33	100±40			103 800±190	1000±300	203	1

the data were converted to  $(T, \sigma)$ , transmission and cross section, vs channel energy for subsequent analysis.

The detailed level analysis was first carried out using our standard transmission dip area analysis<sup>1</sup> which is independent of the resolution width and includes the effect of Doppler level broadening. The levels having shape asymmetry were treated as  $s$  levels, the others as  $p$  levels.

For the  $l=0$  resonances, the area analysis is complicated by the fact that as the level strength is increased, the destructive interference term between potential and resonance scattering on the low side of the resonance tends to give a negative area contribution balancing the positive interference

contribution on the high side. For a given transmission dip area, this can lead to considerable uncertainty in the favored  $g\Gamma_n$  and  $\Gamma$ . To aid in this determination, we also calculated the implied  $T$  vs  $E$  shape for each strong  $s$  level for a series of  $\Gamma$  values for each choice of  $A$  and  $J$ , using  $\Gamma_n \gg \Gamma_\gamma$ , for a shape comparison with our thick natural Tl transmission data. This shape fit, which included Doppler broadening, was mainly responsible for our final level parameter choices in these cases. The level energy  $E_0$  for an  $s$  level is chosen where the resonance contribution to the phase shift is  $90^\circ$  rather than where the total phase shift is  $90^\circ$ . This places  $E_0$  slightly below the energy of the net  $90^\circ$  phase shift by an amount  $\Delta E \approx \frac{1}{2}\Gamma[(1-a)/$

TABLE III. Resonance  $E_0$  and  $ag\Gamma_n$  values for Tl  $l=1$  levels above 20 keV.

$E_0$ (eV)	$ag\Gamma_n$ (eV)	$E_0$ (eV)	$ag\Gamma_n$ (eV)	$E_0$ (eV)	$ag\Gamma_n$ (eV)
21 084±17	2.0 ± 0.9	36 440± 38	3.2±1.4	57 718± 76	6.6± 2.7
21 832±18	0.70±0.25	40 127±44	3.7±1.6	64 308± 90	12 ± 5
22 482±19	0.75±0.27	40 281±45	4.5±2.0	64 757± 91	24 ± 11
22 932±19	1.0 ± 0.4	41 250±46	2.8±1.1	66 507± 94	12 ± 5
23 642±20	2.9 ± 1.4	43 594± 50	4.0±1.6	68 133± 98	17 ± 7
26 767±24	2.5 ± 1.2	43 920± 51	8.5±4.0	75 200±120	35 ± 14
28 689±27	2.5 ± 1.2	44 122± 51	11 ± 4	76 130±120	32 ± 13
28 903±27	1.7 ± 0.7	44 919± 52	7.8±3.4	78 060±120	31 ± 13
30 530±29	1.0 ± 0.4	47 816± 58	10 ± 4	78 780±120	21 ± 8
31 779±31	1.9 ± 0.8	48 481± 59	4.9±2.1	79 640±130	41 ± 16
32 393±32	3.9 ± 1.8	48 922± 60	2.6±1.0	81 640±130	11 ± 5
34 119±35	5.9 ± 2.8	49 340± 60	7.8±3.5	89 370±150	44 ± 17
34 432±35	8.3 ± 4.0	49 775± 61	2.1±0.8	98 760±170	29 ± 12
34 820±36	3.1 ± 1.4	51 831± 65	10 ± 4	101 530±180	54 ± 20
35 987±38	2.5 ± 1.1	53 826± 69	10 ± 4		

$(1+a)]^{1/2}$ , where  $a = \cos 2kR'$ , and  $4\pi\lambda^2 \sin^2 kR'$  is the net potential scattering.

### III. RESULTS AND DISCUSSION

The results for the level parameters for  $^{203}\text{Tl}$  and  $^{205}\text{Tl}$  below 20 keV are given in Table I. We list  $E_0$ ,  $g\Gamma_n$ , and resonance  $l$  choices in all cases, and resonance  $J$  where established. In addition, we established  $\Gamma_\gamma = (0.80 \pm 0.20)$ ,  $(0.54 \pm 0.12)$ ,  $(0.80 \pm 0.16)$ ,  $(0.60 \pm 0.18)$ ,  $(0.65 \pm 0.20)$ , and  $(0.60 \pm 0.20)$  eV for the levels in  $^{203}\text{Tl}$  at 238.0, 842.0, 1433.2, 2790.7, 5813.7, and 6334.2 eV. We obtained  $\Gamma_\gamma = (0.72 \pm 0.18)$  eV for the  $^{205}\text{Tl}$  level at 3039 eV, and  $(0.88 \pm 0.30)$  eV for the level at 5098.4 eV. All of these resonances were "seen" in our thick natural Tl transmission results. When no symbol appears before the energy in Table I, the isotope identification is from our separated isotope results. The isotope identification for levels with \* before the energy is from Ref. 20. The  $^{203}\text{Tl}$  levels having † before the energy were not seen in our separated isotope results but are classified as due to  $^{203}\text{Tl}$  since they were not in the list of  $^{205}\text{Tl}$  levels in Ref. 22.

The  $l=0$  resonances above 20 keV are listed in Table II, giving  $E_0$  and  $\Gamma$  in each case, and values of  $A$  and  $J$  where established. The levels where a "†" is before the  $A$  value had  $A$  established by their observation in our separated isotope results. For the other cases, the best  $A$  is from the best shape fit choice of  $(ag)$  which is 0.074 or 0.221 for  $^{203}\text{Tl}$ ,  $J=0$  or 1, respectively, and 0.176 or 0.529 for  $^{205}\text{Tl}$ ,  $J=0$  or 1, respectively. In these cases, we also established the favored  $J$  of the resonance. Label D before the energy indicates that the level is possibly a doublet.

The levels above 20 keV considered to be  $l=1$  have no  $A$  or  $J$  evaluation. Table III lists the energies and  $ag\Gamma_n$  values for these resonances. Not included are levels seen at 71.67, 72.20, 72.74, 73.17, 73.60, 84.80, 85.96, and 86.93 keV for which meaningful  $ag\Gamma_n$  values could not be obtained.

Figures 1(a)–1(c) show the measured cross section vs energy for the thick natural Tl sample, in the lower part of the figures, for  $\sigma < 30$  b/atom. The upper parts where  $\sigma > 30$  b/atom are for the  $^{203}\text{Tl}$  or  $^{205}\text{Tl}$  isotope samples and give the isotopic cross sections. Most of the isotopic resonance points are due to  $^{203}\text{Tl}$  levels, denoted +. The fewer  $^{205}\text{Tl}$  levels use □ for the cross section points. To avoid misleading statistical noise fluctuations, the  $\sigma$  vs  $E$  tables were first studied to decide which structure was due to true resonances, and which due to statistical fluctuations. In Fig. 1(a), below 1 keV, 50 to 100 channel averages

were used, except near resonances where mainly 5 channel averages were used except at the resonance maxima. In Fig. 1(b) for  $E$  from 1 to 20 keV, we used 5 to 100 channel averages between resonances, with 5 or fewer channel averages near resonance. The plot of Fig. 1(c) uses 1 to 10 channel averages. The between level cross sections stay near 10 b/atom except in the wings of strong  $s$  levels. Our processed data in a format of sample cross section vs energy without any average, are on file at the National Neutron Cross Section Center at Brookhaven National Laboratory.

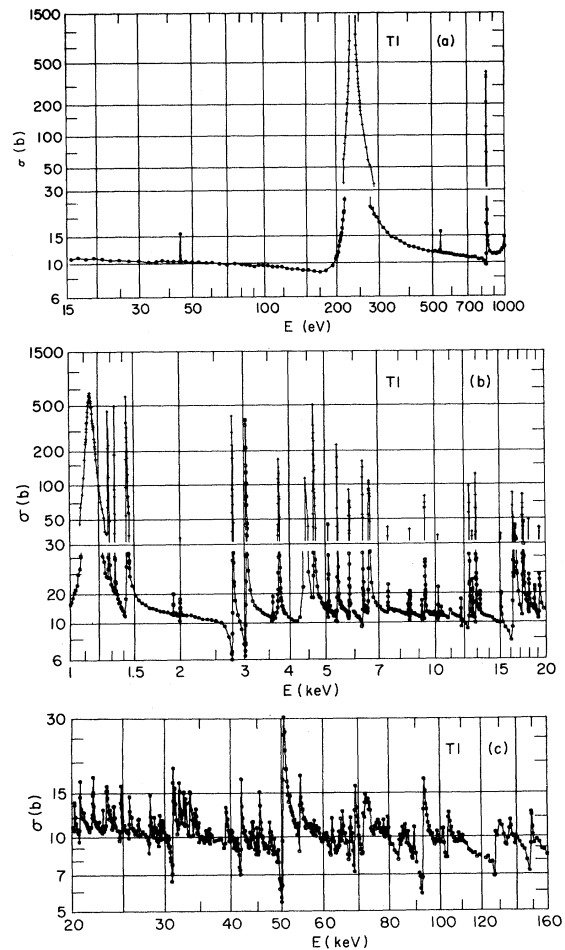


FIG. 1. The measured Tl cross section vs energy (a) below 1 keV, (b) from 1 to 20 keV, and (c) from 20 to 160 keV. The points below 30 b/atom are for natural Tl from the thick natural Tl sample transmission vs energy. The points above 30 b/atom are either  $^{203}\text{Tl}$  or  $^{205}\text{Tl}$  isotope cross sections from the separated isotope sample data. Multichannel data averages were used as appropriate between levels to reduce the statistical fluctuations and the otherwise unacceptable data point clutter (see the text). The resonance points above 30 b/atom are mainly due to  $^{203}\text{Tl}$  and are denoted by †. The  $^{205}\text{Tl}$  points use □ for the cross section points.

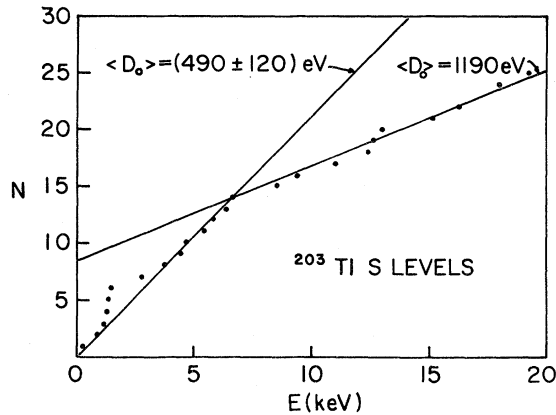


FIG. 2. Plot of the cumulative number  $N$  of observed  $s$  levels in  $^{203}\text{Tl}$  vs energy below 20 keV.

Figure 2 shows the cumulative number  $N$  of observed  $s$  levels in  $^{203}\text{Tl}$  vs  $E$  below 20 keV. Except for the anomalous grouping of four levels between 1.13 and 1.43 keV, the figure splits into two regions, that to 6.6 keV, where  $\langle D_0 \rangle = 490$  eV, and that from 6.6 to 19.23 keV, where the average observed spacing is  $\sim 1190$  eV.

Figure 3 shows  $\sum g\Gamma_n^0$  vs  $E$  for  $^{203}\text{Tl}$  below 20 keV. This also divides into the region below 6.6 keV where a slope  $10^4 S_0 = 2.15 \pm 0.72$  fits best, and the region above 6.6 keV where the slope is about  $0.84 \pm 0.28$ . They are different by more than their combined uncertainty. If the region above 6.6 keV was mainly characterized by missed weak  $s$  levels, it should have its  $\sum g\Gamma_n^0$  slope very little influenced and be the same as below 6.6 keV within statistical uncertainties.

Figure 4 shows two integral plots of the number of levels having  $(g\Gamma_n^0)^{1/2}$  greater than the abscissa

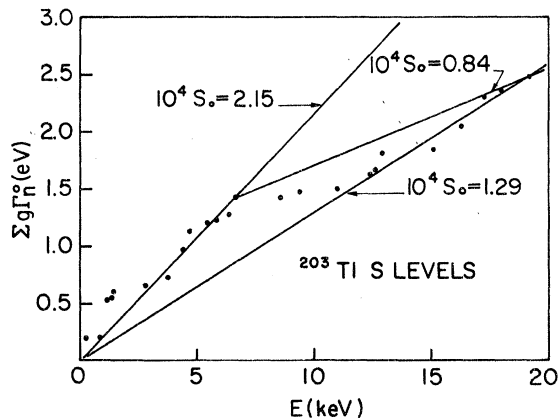


FIG. 3. Plot of  $\sum g\Gamma_n^0$  vs  $E$  for  $^{203}\text{Tl}$ . The quite different mean slopes for  $E < 6.6$  keV and  $E > 6.6$  keV are suggestive of intermediate structure effects.

value, one for  $E < 6.6$  keV, and one for  $E > 6.6$  keV. These plots are remarkable in suggesting that probably only rather weak levels were missed in each interval, with  $\sim 18$  true  $s$  levels appropriate to each interval even though the energy interval is very nearly twice as large for  $E > 6.6$  keV than for  $E < 6.6$  keV. The theoretical Porter-Thomas (PT) single channel fit curves fitted the measured  $\sum g\Gamma_n^0$  for each interval, with the expected true number  $n$  of  $s$  levels for the interval an adjustable parameter. Below 6.6 keV, PT curves are shown for  $n=15$  and  $n=18$ . For  $E > 6.6$  keV, PT curves are shown for  $n=15$ , 18, and 34. In both intervals, the choice  $n=18$  gives a good fit. The curve for  $n=34$  implies the same  $\langle D_0 \rangle$  in the upper region as the fit using  $n=18$  below 6.6 keV. It is seen that the choice  $n=34$  gives a quite poor fit above 6.6 keV even for the upper 70% of the histogram using either  $\sum g\Gamma_n^0/\Delta E$  from the region above 6.6 keV (left curve) or for  $E < 6.6$  keV (right curve). The results for the two regions seem to be incompatible with a common  $\langle D \rangle$  and  $\langle g\Gamma_n^0 \rangle$  for the full interval, thereby suggesting that intermediate structure effects in  $S_0$  vs  $E$  are present. The best choice,  $n=18$  for both regions, gives  $\langle D \rangle = 370 \pm 51$  eV for  $E < 6.6$  keV and  $\langle D \rangle = 700 \pm 97$  eV for  $E > 6.6$  keV. We have no explanation for the different choices of favored  $\langle D \rangle$  for the two energy intervals.

Ignoring the above features, the usual analysis

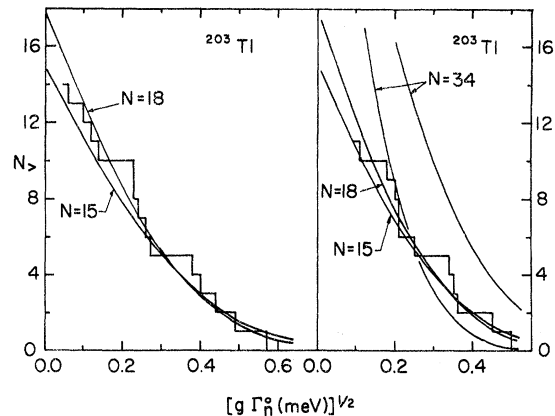


FIG. 4. Plots for  $E < 6.6$  keV (left) and  $6.6 \text{ keV} < E < 20$  keV (right) of the number of observed  $s$  levels in  $^{203}\text{Tl}$  having  $(g\Gamma_n^0)^{1/2}$  greater than the abscissa. Except for the rightmost smooth curve, the fitted curves are single channel Porter-Thomas fits adjusted to the observed  $\sum g\Gamma_n^0$  for each interval separately. Relatively good fits are obtained for 15 and 18 total levels below 6.6 keV and for  $6.6 \text{ keV} < E < 20$  keV. The implied  $\langle D_0 \rangle$  for 18 levels below 6.6 keV implies that 34 levels are expected for  $6.6 \text{ keV} < E < 20$  keV. This curve normalized to the observed  $\sum g\Gamma_n^0$  for the upper region is shown and gives a poor fit. The rightmost curve, for 34 levels, and the implied  $S_0$  below 6.6 keV, is also a very poor fit.

below 20 keV would give  $10^4 S_0 = (1.28^{+0.45}_{-0.31})$  for  $^{203}\text{Tl}$  and  $(0.38^{+0.44}_{-0.18})$  for  $^{205}\text{Tl}$ . Values  $10^4 S_1 = (0.25^{+0.16}_{-0.09})$  and  $(0.15^{+0.14}_{-0.07})$  are obtained for  $^{203}\text{Tl}$  and  $^{205}\text{Tl}$ , respectively, ignoring possible contributions of missed weaker  $p$  levels. A channel radius  $R = 1.4A^{1/3} \text{ fm} = 8.23 \text{ fm}$  is used to obtain the  $g\Gamma_n^1$  and  $S_1$  values.

We wish to thank Dr. H. S. Camarda, Dr. F. Rahn, Dr. M. Slagowitz, and Dr. S. Wynchank for their involvement in the measurements. The support by C. Gillman and W. Marshall was important. We thank Dr. George Rogosa and his colleagues at the Atomic Energy Commission for help in obtaining the separated isotope samples.

†Research supported by the U. S. Atomic Energy Commission.

\*Present address: Brookhaven National Laboratory, Upton, New York 11973.

- <sup>1</sup>H. I. Liou *et al.*, Phys. Rev. C 5, 974 (1972), Er.  
<sup>2</sup>F. Rahn *et al.*, Phys. Rev. C 6, 251 (1972), Sm, Eu.  
<sup>3</sup>F. Rahn *et al.*, Phys. Rev. C 6, 1854 (1972),  $^{232}\text{Th}$ ,  $^{238}\text{U}$ .  
<sup>4</sup>H. I. Liou *et al.*, Phys. Rev. C 7, 823 (1973), Yb.  
<sup>5</sup>H. S. Camarda *et al.*, Phys. Rev. C 8, 1813 (1973), W.  
<sup>6</sup>F. Rahn *et al.*, Phys. Rev. C 8, 1827 (1973), Na.  
<sup>7</sup>U. N. Singh *et al.*, Phys. Rev. C 8, 1833 (1973), K.  
<sup>8</sup>H. I. Liou *et al.*, Phys. Rev. C 10, 709 (1974), Cd.  
<sup>9</sup>G. Hacken *et al.*, Phys. Rev. C 10, 1910 (1974), In.  
<sup>10</sup>F. Rahn *et al.*, Phys. Rev. C 10, 1904 (1974), Gd.  
<sup>11</sup>U. N. Singh *et al.*, Phys. Rev. C 10, 2138 (1974), Cl.  
<sup>12</sup>U. N. Singh *et al.*, Phys. Rev. C 10, 2143 (1974), Ca.  
<sup>13</sup>U. N. Singh, H. I. Liou, J. Rainwater, G. Hacken, and J. B. Garg, Phys. Rev. C 10, 2147 (1974), F.  
<sup>14</sup>U. N. Singh, H. I. Liou, J. Rainwater, G. Hacken, and J. B. Garg, Phys. Rev. C 10, 2150 (1974), Mg.

- <sup>15</sup>H. I. Liou, G. Hacken, J. Rainwater, and U. N. Singh, Phys. Rev. C 11, 462 (1975), Dy.  
<sup>16</sup>H. I. Liou, J. Rainwater, G. Hacken, and U. N. Singh, Phys. Rev. C 11, 457 (1975), Ar.  
<sup>17</sup>H. I. Liou, J. Rainwater, G. Hacken, and U. N. Singh, Phys. Rev. C 11, 1231 (1975),  $^{175}\text{Lu}$ .  
<sup>18</sup>U. N. Singh, J. Rainwater, H. I. Liou, G. Hacken, and J. B. Garg, Phys. Rev. C 11, 1117 (1975), Al.  
<sup>19</sup>H. I. Liou, J. Rainwater, G. Hacken, and U. N. Singh, Phys. Rev. C 11, 2022 (1975),  $^{177}\text{Hf}$ .  
<sup>20</sup>*Neutron Resonance Parameters*, compiled by S. F. Mughabghab and D. I. Garber, Brookhaven National Laboratory Report No. BNL-325 (National Technical Information Service, Springfield, Virginia, 1973), 3rd ed., Vol. I.  
<sup>21</sup>H. W. Newson *et al.*, Ann. Phys. (N.Y.) 14, 346 (1961).  
<sup>22</sup>E. D. Earle *et al.*, in *Statistical Properties of Nuclei*, edited by J. B. Garg (Plenum, New York, 1972), pp. 263–270.  
<sup>23</sup>E. D. Earle *et al.*, Bull. Am. Phys. Soc. 19, 574 (1974).